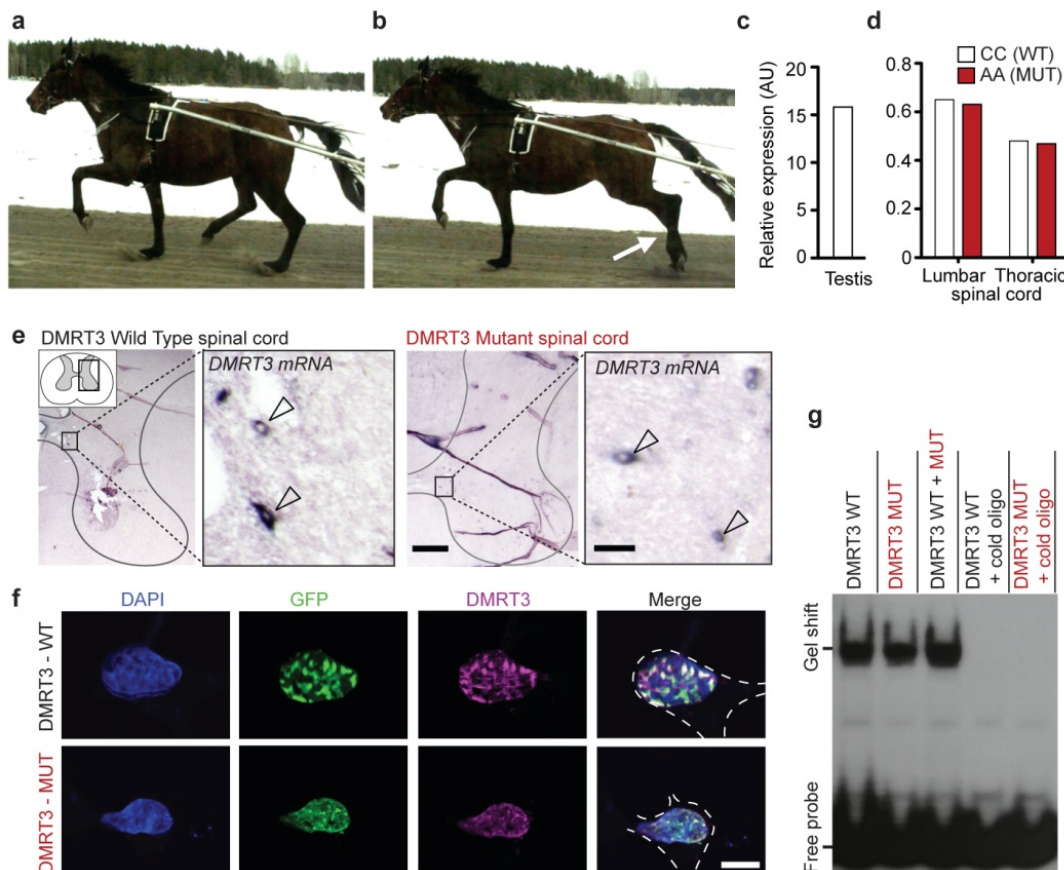
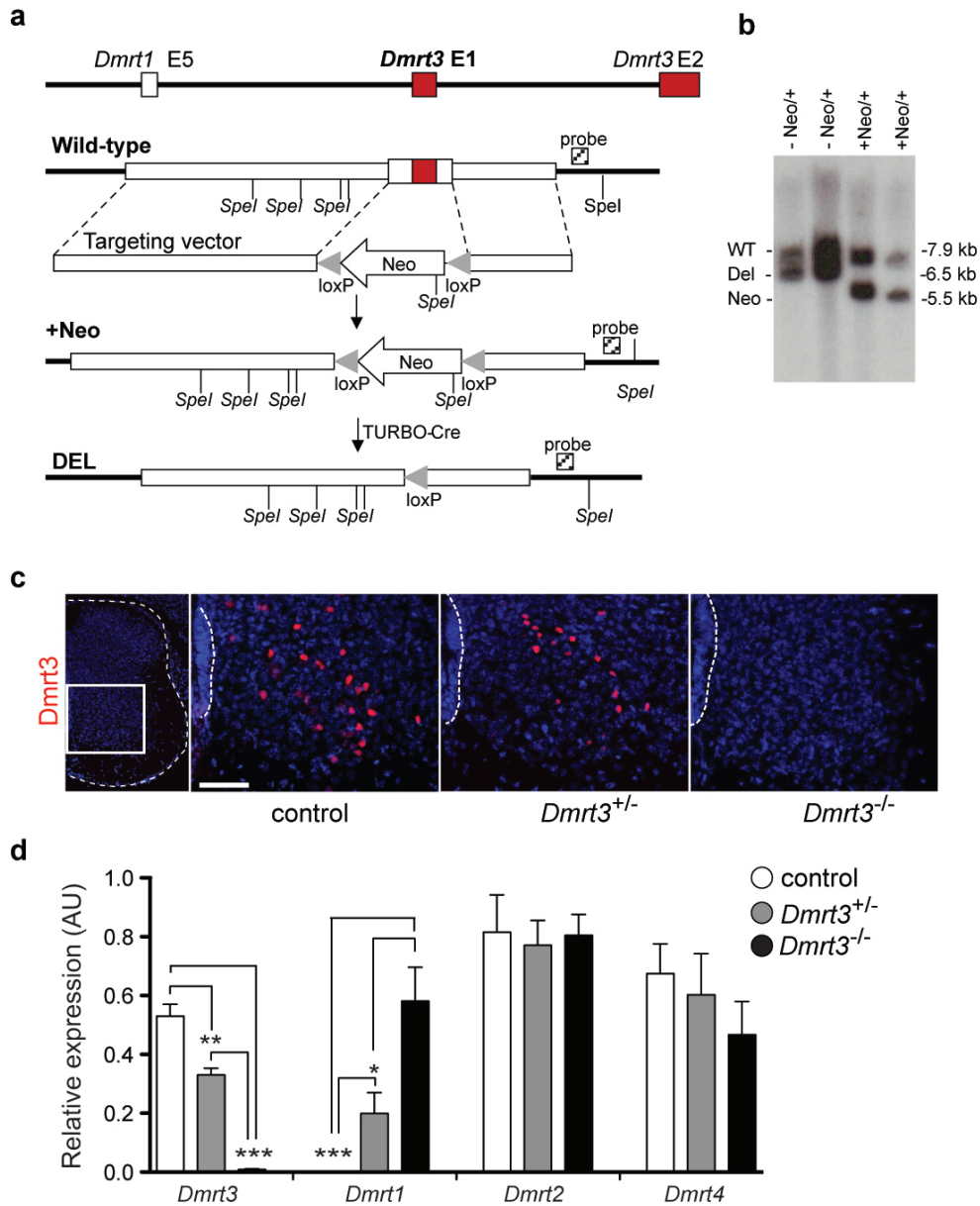


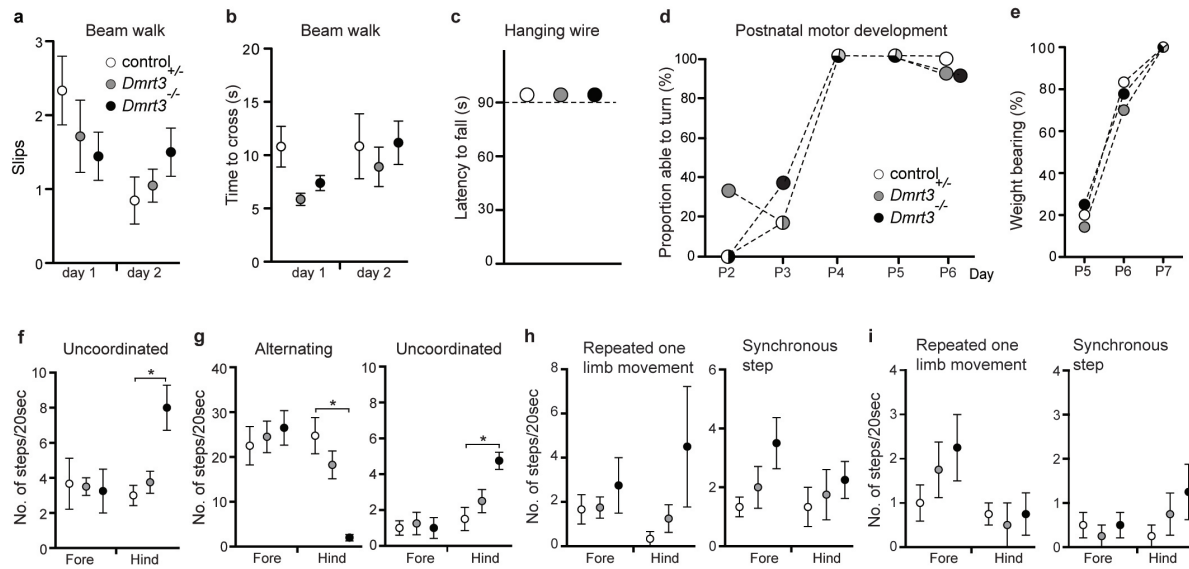
## Supplementary figures and figure legends



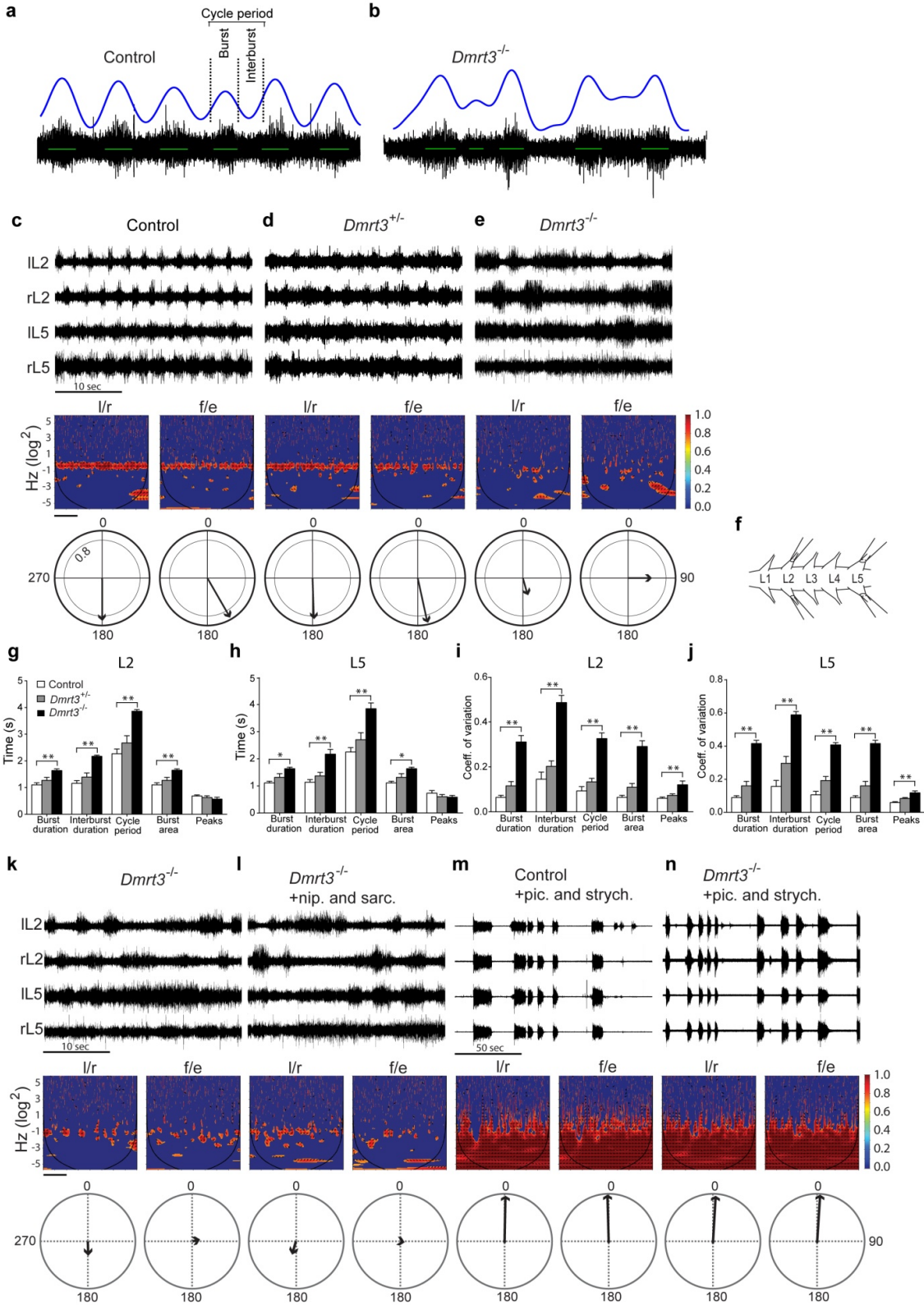
**Supplementary Figure 1. Asymmetric trot in a *DMRT3* heterozygous horse and functional characterization of the horse *DMRT3* mutation.** **a,b**, Images illustrating asymmetric diagonal trot of a heterozygous (CA) Standardbred horse close to transition into canter (images taken at equivalent stride positions, time delay 260 ms). Note the large difference in position of the hind limbs (arrow) in relation to the diagonal front legs, which in a symmetric trot should be equal. **c**, Real-time qPCR for *DMRT3* mRNA in testis from wild type (CC, n=1) horse compared to housekeeping genes, expressed in arbitrary units (AU). **d**, Relative mRNA expression of *DMRT3* in lumbar and thoracic spinal cord of wild type (CC, n=4) and mutant (AA, n=1) horse. **e**, RNA *in situ* hybridization of tissue sections from the lumbar spinal cord of wild-type (CC, left) and mutant (AA, right) horse. Arrows mark neurons with *DMRT3* expression. **f**, Transfection experiments in human glioma U251 cells. eGFP-*DMRT3* proteins (green) corresponding to the wild-type and mutant forms coincides with anti-*DMRT3* antibody labeling (purple), both showing nuclear localization (co-localization with DAPI, blue), consistent with the presence of a conserved nuclear localization signal (KGHKR) in the DM domain of *DMRT3*<sup>28</sup>. **g**, Electrophoretic mobility shift assays using an oligonucleotide containing a *DMRT3*-binding motif<sup>29</sup> and *in vitro*-translated myc-tagged *DMRT3* wild-type and mutant proteins. An oligonucleotide containing a *DMRT1*-binding site was also used and gave similar results (data not shown). The cold competing oligonucleotide was added in 150x excess. Scale bars: 1 mm (**e**), 100  $\mu$ m (**e**, close-up), 10  $\mu$ m (**f**).



**Supplementary Figure 2. Generation and characterisation of the *Dmrt3* null mutant mouse.** **a**, The *Dmrt3* mouse genomic region (top), the wild-type allele, the Neo insertion (+Neo) and the Neo deletion (DEL) allele for each element are shown successively (figures not drawn to scale). The points of integration of target vector homology arms and the probe (striped box; chr19:25,688,502-25,688,838;mm9) used in the Southern hybridization for identification of embryonic stem (ES) cells carrying the deletion together with the restriction sites are shown. **b**, Southern blot showing the Neo inserted (+Neo/+) and Neo deleted (-Neo/+) ES cells following *SpeI* digestion. **c**, Transverse spinal cord sections of wild-type control, *Dmrt3*<sup>+/-</sup> and *Dmrt3*<sup>-/-</sup> E15.5 mice according to the white box, with the area of higher magnification in panels to the right, show absence of *Dmrt3* immunolabelling in the *Dmrt3*<sup>-/-</sup> spinal cord. Scale bar 70  $\mu$ m. **d**, Relative mRNA expression levels of *Dmrt* genes, *Dmrt1-4*, in the lumbar region of mouse spinal cord (Control n=8, *Dmrt3*<sup>+/-</sup> n=4 and *Dmrt3*<sup>-/-</sup> n=6, >2 weeks old). No expression of *Dmrt3* was detected in *Dmrt3*<sup>-/-</sup> and lower levels of *Dmrt3* in *Dmrt3*<sup>+/-</sup> ( $P < 0.0001$ ) compared to control. *Dmrt1* expression was up regulated in *Dmrt3*<sup>-/-</sup> and *Dmrt3*<sup>+/-</sup> ( $P < 0.0001$ ). Mean  $\pm$  s.e.m.

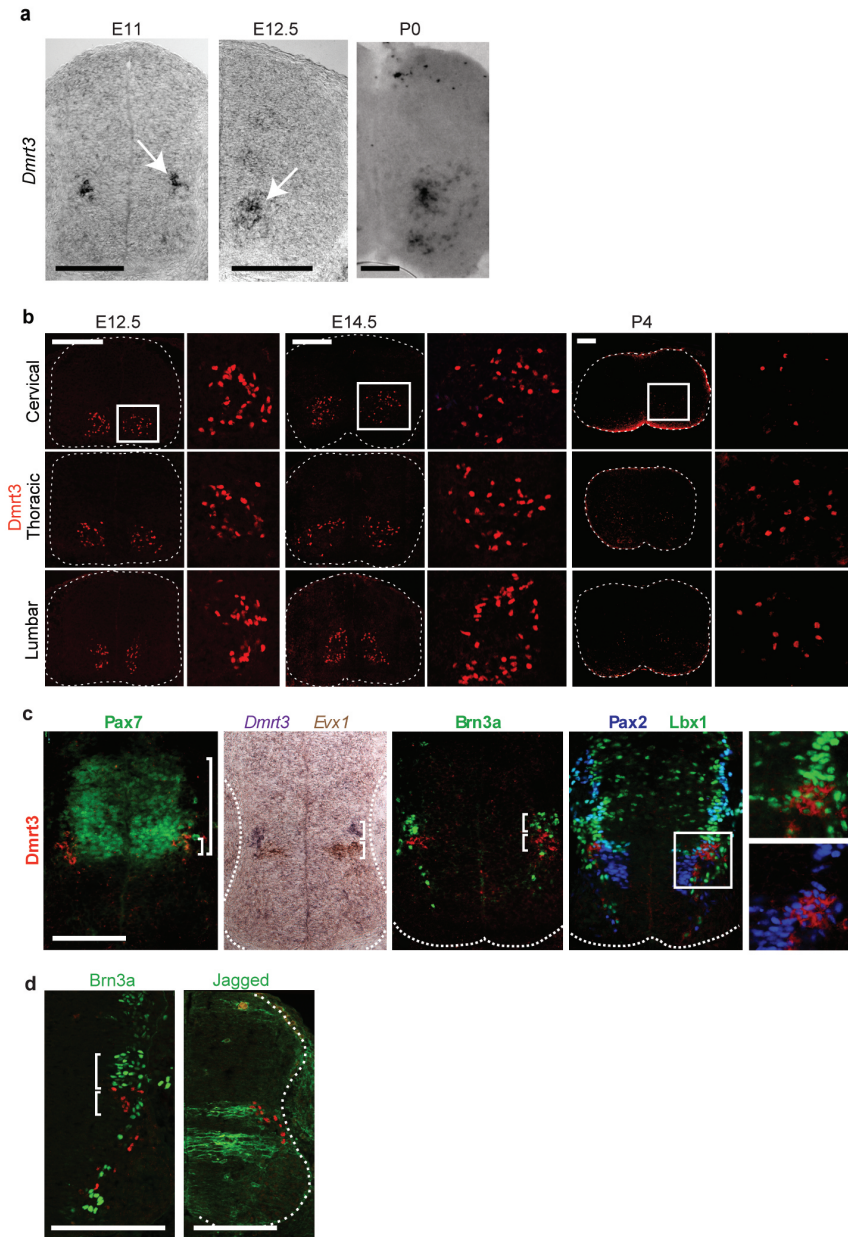


**Supplementary Figure 3. Characterisation of motor behaviour.** **a**, No difference in fine motor coordination was observed between genotypes in adult mice scored for the number of hind limb slips in a beam-walking test (n=5 control and  $Dmrt3^{-/-}$ , n=7  $Dmrt3^{+/-}$ ). **b**, The latency to cross the beam in the beam walking test was similar between genotypes (n=5 control, n=7  $Dmrt3^{+/-}$ , n=6  $Dmrt3^{-/-}$ , 3 trials/mouse per day). **c**, Muscle function was evaluated using the four limb hanging wire test. All animals (n=5/genotype) managed to hang for >90 s. **d**, Postnatal locomotor development in newborn mice between postnatal day 2 and day 6 were analysed by the ability to turn over from their backs. Each animal was given two trials per day. No major difference between genotypes was seen (P2-P5: n=3 wild type control, n=3  $Dmrt3^{+/-}$ , n=4  $Dmrt3^{-/-}$ , P6: n=5 control, n=7  $Dmrt3^{+/-}$ , n=6  $Dmrt3^{-/-}$ ). **e**, Weight-supported movements developed at similar postnatal time points between genotypes, by postnatal day 5 (P5): control 20% (n=5),  $Dmrt3^{+/-}$  14% (n=4) and  $Dmrt3^{-/-}$  25% (n=8) and by P6: control 83% (n=6),  $Dmrt3^{+/-}$  70%, (n=10) and  $Dmrt3^{-/-}$  78%, (n=9). All mice walked at P7 independent of genotype. **f,g,h,i** Performance of Uncoordinated, Alternating, Repeated one limb movement and Synchronous limb movement in airstepping for P4 and P1 mice. At P4 (**f**) as well as at P1 (**g**)  $Dmrt3^{-/-}$  mice showed an increased number of uncoordinated steps (P=0.029; P4 and P=0.026; P1) in their hindlimbs and a decreased number of alternating steps (P=0.02). No differences were observed in the number of Repeated one limb movement or Synchronous step at either P4 (**h**) or at P1 (**i**). (n=4/genotype, except at P4: n=3 for controls). Wild-type littermate controls (white),  $Dmrt3^{+/-}$  (grey),  $Dmrt3^{-/-}$  (black). Mean  $\pm$  s.e.m..



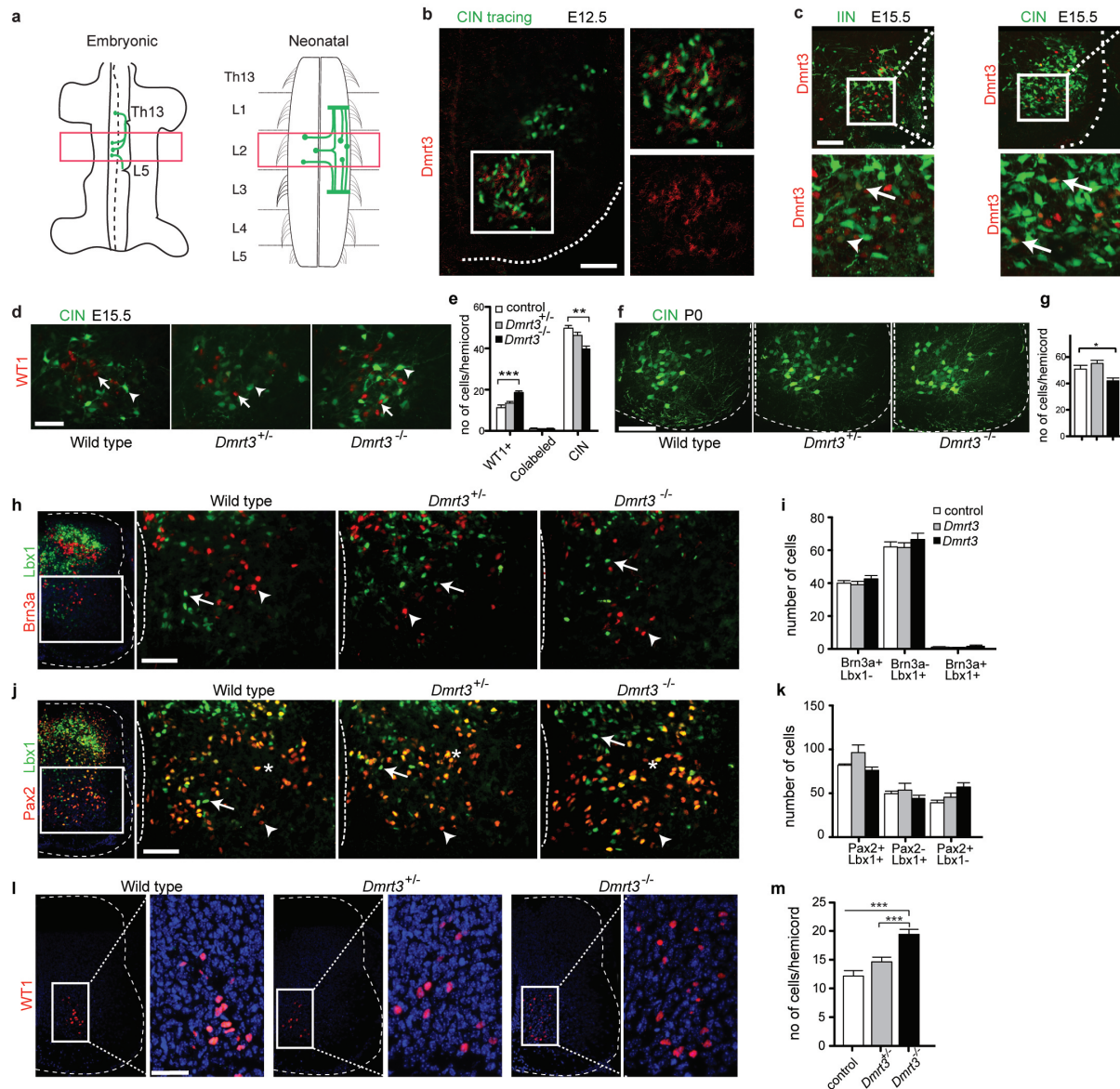
Supplementary Figure 4

**Supplementary Figure 4. Electrophysiological analysis and effect of adding nipecotic acid and sarcosine or picrotoxin and strychnine.** **a**, Examples of wild-type control and **b**,  $Dmrt3^{-/-}$ , raw traces of ventral root fictive locomotion. In blue, high-pass filtered, rectified and low-pass filtered raw traces of recordings. Burst duration, interburst duration and cycle period are marked in the blue trace. **c,d,e**, Representative traces from control (**c**),  $Dmrt3^{+/-}$  (**d**) and  $Dmrt3^{-/-}$  (**e**) spinal cords. Time scale 10 s. Analysis was done using coherence power spectra and phase analysis of left/right and flexor/extensor recordings. Coherency regions around 0.4 Hz emerged for control and for  $Dmrt3^{+/-}$  mice (red) but was absent in  $Dmrt3^{-/-}$  spinal cord recordings (color-graded scale). Time scale 100 s. Phase analysis of 600 seconds of recorded traces (circular plots) show that control and  $Dmrt3^{+/-}$  mice displayed patterns of left/right and flexor/extensor alternation while traces from  $Dmrt3^{-/-}$  spinal cords were uncoordinated. For the circular plots: a value close to 180 indicates alternating coordination, the length of the arrow is a measure of statistical significance of the preferred phase. Arrows represent the mean,  $n=6$ /genotype, wild-type (l/r avg phase preference,  $179.9^\circ$ ,  $R=0.88$ ; f/e  $150.0^\circ$ ,  $R=0.94$ ),  $Dmrt3^{+/-}$  (l/r,  $178.1^\circ$ ,  $R=0.84$ ; f/e  $167.7^\circ$ ,  $R=0.94$ ),  $Dmrt3^{-/-}$  (l/r,  $164.56^\circ$ ,  $R=0.33$ ; f/e  $90^\circ$ ,  $R=0.48$ ). **f**, Schematic of an isolated spinal cord with attached suction electrodes to record the rhythmic ventral root activities (fictive locomotion) from left (l) and right (r) lumbar (L) root 2 and 5. Application of serotonin and N-methyl-D-aspartate initiates fictive locomotion from L2 (primarily flexor) and L5 (primarily extensor) lumbar ventral roots allowing for evaluation of left/right and flexor/extensor coordination. **g,h**, Analysis of fictive locomotion from control,  $Dmrt3^{+/-}$  and  $Dmrt3^{-/-}$  spinal cords show a consistent increase in burst duration, interburst duration, cycle period and burst area measured in the L2s as well as in the L5s of the  $Dmrt3^{-/-}$  compared to control. **i,j**, The coefficient of variation, a normalized measure of variability of a probability distribution, increased for burst duration, interburst duration, cycle period and burst area in both L2 and L5 in  $Dmrt3^{-/-}$  spinal cords compared to control ( $n=6$ /genotype, for the L2: burst duration  $**P=0.0097$ , interburst duration  $**P=0.0028$ , cycle period  $**P=0.0028$ , burst area  $**P=0.0070$ ; L2 coefficient of variation: burst duration  $**P=0.0015$ , interburst duration  $**P=0.0023$ , cycle period  $**P=0.0019$ , burst area  $**P=0.0015$ , peaks  $**P=0.0065$ ; L5: burst duration  $*P=0.016$ , interburst duration  $**P=0.0030$ , cycle period  $**P=0.0050$ , burst area  $*P=0.016$ , L5 coefficient of variation: burst duration  $**P=0.0011$ , interburst duration  $**P=0.0013$ , cycle period  $**P=0.0013$ , burst area  $**P=0.0011$ , peaks  $**P=0.0030$ , Kruskal-Wallis test). **k**, A representative trace from a  $Dmrt3^{-/-}$  spinal cord bathed in a cocktail of serotonin and N-methyl-D-aspartate in order to induce fictive locomotion. **l**, In order to strengthen inhibition across the midline in an attempt to compensate for the loss of the inhibitory  $Dmrt3$  neurons, GABA and glycine uptake blockers nipecotic acid and sarcosine and recorded locomotor activity were applied. Time scale represents 10 seconds. Coherence power spectra of left/right and flexor/extensor recordings (color-graded scale) and phase analysis of 600 seconds of recorded traces (circular plots) showed that treatment with nipecotic acid and sarcosine did not result in an improved degree of coherency between either left/right or flexor/extensor ventral root activities ( $n=3$ ). **m,n**, In order to examine if  $Dmrt3^{-/-}$  has an effect on the coordination of solely excitatory communication over the midline, we treated spinal cords of control and  $Dmrt3^{-/-}$  mice with the GABA<sub>A</sub> receptor antagonist picrotoxin and the glycine receptor antagonist strychnine. In the control, a slow synchronous rhythm appears and we also detect the same pattern in the  $Dmrt3^{-/-}$  spinal cords. Time scale 100 seconds. Mean  $\pm$  s.e.m..



**Supplementary Figure 5. Characterisation of *Dmrt3* expressing cells in the mouse spinal cord.**

**a**, *Dmrt3* mRNA expression was detected on spinal cord sections from embryonic and postnatal ages as indicated. **b**, *Dmrt3* immunopositive cells were found at cervical, thoracic and lumbar levels at E12.5, E14.5 and P4. **c**, *Dmrt3* mRNA expression was detected using *in-situ* hybridisation and was combined with immunohistochemical stainings using antibodies specific for different neuronal populations in the spinal cord during development (E11.5). *Dmrt3* mRNA expression (red) was found in the ventral most part of the dorsal progenitor domain Pax7 (green). *Dmrt3* mRNA (purple) did not overlap with the V0<sub>v</sub>/V0<sub>c</sub>/V0<sub>G</sub> marker Evx1 (orange) or with the dI1/dI2/dI3/dI5 marker Brn3a (green). Pax2 (blue) is expressed in dI4/dI6/V0d populations and Lbx1 (green) is expressed in dI4/dI5/dI6 and both showed an overlapping expression with *Dmrt3* mRNA expression. A schematic illustration of a spinal cord cross section showing the location of expression of progenitor domains and transcription factors used to characterize *Dmrt3* is found in Fig. 3c. **d**, *Dmrt3*<sup>+</sup> cells do not overlap with the dI1/dI2/dI3/dI5 marker Brn3a (compare brackets) but originate from the same domain as the dI6/V1/V2 marker Jagged. Scale bars: 80 μm.



**Supplementary Figure 6. Analysis of spinal interneuron subpopulations on spinal cords from control, *Dmrt3*<sup>+/-</sup> and *Dmrt3*<sup>-/-</sup> mice. a-g**, Tracing analysis of spinal interneurons. **a**, Schematic drawings of the Fluorescein-dextran amine (FDA) application sites and the area of analysis (box). **b**, FDA commissural interneuron retrograde labelling at E12.5 showed that cells positive for *Dmrt3* mRNA expression (red) intermingled, but did not overlap with the medioventral population of the traced commissural interneurons (CIN, green). **c**, Retrograde labelling in E15.5 spinal cords indicate that *Dmrt3*<sup>+</sup> interneurons extend projections both ipsilateral (IIN) and contralateral. Arrows point to *Dmrt3*<sup>+</sup> interneurons also positive for the tracer (green). **d**, WT1 staining (arrows) with CIN FDA tracing (arrowheads) at E15.5. **e**, Quantification of WT1<sup>+</sup> neurons and CINs at E15.5 (2 animals/genotype; control n=10 sections, *Dmrt3*<sup>+/-</sup> n=11 sections, *Dmrt3*<sup>-/-</sup> n=20 sections, \*\*P=0.0013). **f**, Retrograde labelling in P0 spinal cords indicate a decrease of CIN in the *Dmrt3*<sup>-/-</sup>. **g**, Quantification of one segment (L2) projecting CIN at P0-P2 (3 animals/genotype; control n=10 sections, *Dmrt3*<sup>+/-</sup> n=9 sections, *Dmrt3*<sup>-/-</sup> n=10 sections, \*P=0.0051). The spinal cord is outlined with dashed line and labelling of transcription factors are indicated by colour. **h**, Double immunolabelling of Brn3a (red, arrowheads) and Lbx1 (green, arrows). **i**, Quantification of Brn3a/Lbx1 positive neurons (control n=16 sections, *Dmrt3*<sup>+/-</sup> n=15 sections, *Dmrt3*<sup>-/-</sup> n=21

sections). **j**, Double immunolabelling of Pax2 (red, arrowheads) and Lbx1 (green, arrows), Pax2 and Lbx1 labelled cells (stars). **k**, Quantification of Lbx1/Pax2 positive neurons. No difference between genotypes was found in the number of dI4, dI5, dI6 or V0 neurons labelled by Brn3a, Pax2 and Lbx1 (control n=11 sections, *Dmrt3*<sup>+/-</sup> n=11 sections, *Dmrt3*<sup>-/-</sup> n=19 sections). **l**, Immunolabelling of WT1 (red). **m**, Quantification of WT1 immunopositive neurons demonstrated that loss of *Dmrt3* leads to an increase of the dI6 subpopulation labelled by WT1 (control n=43 sections, *Dmrt3*<sup>+/-</sup> n=36 sections, *Dmrt3*<sup>-/-</sup> n=46 sections, \*\*\*P<0.0001). The region of counted neurons (white boxes) is shown in higher magnification, spinal cord edge (dashed line). Mean ± s.e.m. Scale bars: 70 µm (**b,c,d,h,j**), 100 µm (**f**), 50 µm (**l**).



## Supplementary Methods

### Horses

Samples from Icelandic horses used for the genome-wide analysis were collected in Sweden, with the phenotype of each horse scored through a questionnaire sent out to horse owners. The other gaited breeds, as well as the American Standardbreds, were collected in the US. The remaining anonymous horse samples were from the biobank at the Animal Genetics Laboratory, SLU, Sweden. Breeding field test scores on Icelandic horses were acquired from the Icelandic horse registry WorldFengur ([www.worldfengur.com](http://www.worldfengur.com)) and phenotypic records and estimated breeding values for Swedish Trotters were obtained from the database of the Swedish Trotting Association. Estimated breeding values for harness racing traits in Swedish trotters are computed by the Best Linear Unbiased Prediction (BLUP) method<sup>30</sup>. The estimated breeding values are based on performance data for the total population. The values are adjusted for systematic fixed environmental effects and combine the information from relatives with the horses' own performance results. The published estimated breeding values are scaled so that the value 100 represents the current population average and selection of breeding animals with estimates above this value are thought to lead to genetic improvement of the breed.

### Genome wide association and SNP genotyping

PLINK<sup>31</sup> was used for quality control and association analysis of the SNP data generated using the Illumina EquineSNP50 BeadChip. The chip contains 54,602 SNPs and the average genotyping rate was higher than 0.99. The following numbers of SNPs were excluded after quality control: 409 SNPs with more than 10% missing genotypes, 28 SNPs that departed significantly from Hardy-Weinberg equilibrium ( $P < 10^{-6}$ ) and 14,555 with a minor allele frequency  $< 5\%$ . This left 39,815 SNPs to analyse. We used a full-model association test and permuted P-values 100,000 times to test for significance under a recessive mode of inheritance. A Q-Q plot (not shown) as well as the estimated genomic inflation factor (1.066) did not reveal that stratification was a concern in this material.

A custom TaqMan SNP Genotyping assays (Applied Biosystems) was used to genotype the *DMRT3\_Ser301STOP* mutation with the following primers and probes: forward primer: CCTCTCCAGCCGCTCCT; reverse primer: TCAAAGATGTGCCCGTTGGA; wild-type probe: CTGCCGAAGTTCG; mutant probe: CTCTGCCTAAGTTCG. The ABI PRISM 7900 HT sequence detection system for 384-well format (Applied Biosystems) was used for the analysis. Differences in mean value of earnings, BLUP values and breeding field scores were tested using two-sample equal variance Student's *t*-test.

### Genome resequencing

DNA samples from two Icelandic horses, one female mutant *DMRT3* homozygote and one male control (homozygous wild-type) were prepared for sequencing. Illumina paired-end libraries were generated from these DNA samples with mean insert sizes of approximately 220 bp. The two libraries were sequenced (2 x 100 bp) on seven and five lanes respectively, using an Illumina HiSeq instrument. The reads were mapped to the horse genome (EquCab2 reference assembly) using the software BWA, and PCR-duplicates were removed using the software Picard (<http://picard.sourceforge.net>). The average read depth obtained for each sample was approximately 30x. SNPs and small insertions/deletions were called from the mapping data after subjecting the alignments to realignment around indels and then variant calling using the Genome Analysis Toolkit (GATK)<sup>32</sup>. The variant calls were subjected to recommended VariantFiltrationWalker filters for SNPs listed in the GATK wiki page ([http://www.broadinstitute.org/gsa/wiki/index.php/The\\_Genome\\_Analysis\\_Toolkit](http://www.broadinstitute.org/gsa/wiki/index.php/The_Genome_Analysis_Toolkit)) and read alignments overlapping SNP and insertion/deletion calls within the 438 kb *Gait* locus were then manually reviewed to remove obvious artifact calls. Read depths observed in one kilobase windows were used to call candidate duplications in the minimum IBD region, and mapping distances and

orientations between paired reads were used to detect structural variations in relation to the reference assembly. The software ANNOVAR<sup>33</sup> was used to annotate SNPs in relation to Ensembl genes.

### Mice

*Dmrt3* null mice were generated by deleting a sequence covering exon 1, which includes the start codon and the DM binding domain of *Dmrt3* (chr19:25,684,562-25,686,077; mm9; *Dmrt3*<sup>tm1Hgc</sup>) (Supplementary Fig. 2)<sup>5</sup>. All animals used for experiments were from *Dmrt3* heterozygous breedings. All mice were kept according to the guidelines of Swedish regulation and European Union legislation (ethical permits C350/10, C192/11, C248/11, C91/12). Control mice were always littermates (wild-type; *Dmrt3*<sup>+/+</sup>).

### Immunohistochemistry

The anti-*Dmrt3* antibody was custom made in guinea pig using the immunizing peptide CKQSIYTEDDYDERS-amide (Innovagen, Lund, Sweden). Antibodies were incubated in 5% goat serum, 0.3% BSA in PBS in the following dilutions: mEvx1 1:50 (Developmental Studies Hybridoma Bank, University of Iowa, Iowa City, IA), gpLbx1 1:10,000 (kind gift from C. Birchmeier, MDC, Berlin, Germany), rPax2 1:1000 (Covance), mBrn3a 1:500 (Millipore Bioscience Research Reagents), mPax7 1:100 (Developmental Studies Hybridoma Bank), rbLmx1b 1:2000 (gift from Yu-Qiang Ding), rJagged 1:20 (Developmental Studies Hybridoma Bank), rbWt1 1:500 (Santa Cruz Biotechnology, Inc., Santa Cruz, California, USA), chGFP 1:1000 (Abcam). Quantitative analysis of the antibody staining was statistically analysed using one-way ANOVA followed by Bonferroni's post hoc test.

### RTqPCR

Lumbar spinal cord from 3 weeks old mice (n=6 wild-type, n=4 *Dmrt3*<sup>+/-</sup>, n=4 *Dmrt3*<sup>-/-</sup>) were dissected and snapfrozen. RNA was isolated using RNeasy kit (Qiagen) followed by DNase I treatment (Fermentas) to remove DNA contamination. 0.8 µg of each RNA sample was reverse transcribed using M-MLV reverse transcriptase (Life-technologies) and used for qPCR. Primers for DMRT1, DMRT2, DMRT3 and DMRT4 were designed using Primer3plus and single product formation was evaluated from melting curves for each primer pair (listed in table below). Real time PCR was carried out in triplicates for each sample using KAPA™ SyBr® FAST qPCR Kit (KAPA Biosystems Inc., Woburn, USA) and Bio-Rad iCycler™ (Bio-Rad). PCR efficiencies of primer pairs were calculated by linear regression method (LinRegPCR). Cq values were normalized to the geometric mean of the two most stable reference genes, *Tubulin-beta5* and *Rpl19* tested on geNorm algorithm. Relative expression was determined from normalized Cq values and analysed using one-way ANOVA followed by Bonferroni's post hoc test.

### Adult mouse locomotor behaviour

Adult motor behaviour was analysed in 6-8 week old mice of mixed gender. The body weight of each animal was measured daily since *Dmrt3*<sup>-/-</sup> mice develop dental malocclusions after approximately 2 months of age<sup>5</sup>. Only *Dmrt3*<sup>-/-</sup> mice that had a normal growth curve and without a detectable teeth complication were included in the analysis. The experimenter was blind to genotype while performing and analysing experiments.

Fine motor coordination was evaluated using a beam-walking test. The device consisted of a 1 m long and 12 mm in diameter round wooden beam positioned 35 cm above the ground. Mice were trained on a 24 mm beam before the experiment. Each animal (n=5 control, n=7 *Dmrt3*<sup>+/-</sup>, n=6 *Dmrt3*<sup>-/-</sup>) was analysed three times per day for three days and the number of hind limb slips and latency time was scored (maximum cut of time was 30 s).

Swimming performance was analysed by placing the mouse in a glass cylinder filled with 25 °C water, depth 25 cm (n=5 control and *Dmrt3*<sup>-/-</sup>, n=7 *Dmrt3*<sup>+/-</sup>). Swimming activity was defined as the time spent moving using at least three paws paddling. A mouse was considered immobile

when floating or making occasional paddling movements. A third parameter termed twitching was also recorded, defined as high frequent twitch/cramp-like limb movement without full extension. The duration for each activity was recorded during one minute after placing the mouse in the cylinder.

Gross muscle impairment was evaluated using the hanging wire test. Four limb wire hanging test was performed by placing the mouse on a wired cage top which was slowly inverted 35 cm over a padded cage. The hanging latency time was recorded with a maximum cut of time of 90 s (n=5 control, n=7 *Dmrt3*<sup>+/-</sup>, n=6 *Dmrt3*<sup>-/-</sup>).

Gait analysis was performed using the TreadScan (CleverSys, Reston, VA) apparatus. Mice were acclimatized in the setup and trained at a treadmill speed of 6 cm/s. The analysis was conducted at five speeds 9, 15, 20, 25 and 30 cm/s, repeated for three consecutive days (n=5/genotype; control: 2 males, 3 females, *Dmrt3*<sup>+/-</sup>: 4 males, 1 female, *Dmrt3*<sup>-/-</sup>: 3 males, 2 females). Mice refusing to run were stimulated to do so using a spatula. Recordings at 100 frames/s for 20 s were acquired with the TreadScan software. The ability to maintain locomotion at a certain speed was defined as five complete stride cycles. Segments of 500-1500 frames (corresponding to at least 10 complete step cycles) where the animal displayed continuous locomotion were selected for automated gait analysis using the TreadScan software. Gait analysis was performed at 20 cm/s (n=11-12 trials, 5 animals/genotype) as well as 9 and 15 cm/s (n=4-9 trials, 3 animals/genotype). Recorded steps were manually examined and incomplete and miscalculated steps were excluded. The gait parameters stride, stance, break, propulsion and swing time were automatically calculated and average values for each limb and trial were used for statistical analysis.

TreadScan data was normally distributed and analysed for statistical significance using one-way ANOVA with Bonferroni post-hoc test. The ability to maintain a certain treadmill speed was analysed with Fisher's exact test for the total number of trials (n=15/genotype). One-way ANOVA followed by Bonferroni post-hoc test was used to examine beam-walk and swimming behaviour. Probability values <0.05 were considered statistically significant.

### Postnatal development analysis

Locomotor development was analysed in neonatal control, *Dmrt3*<sup>+/-</sup> and *Dmrt3*<sup>-/-</sup> mice between P2 and P7. The mouse was placed on a flat surface and recorded from the side or above. The ability to turnaround after lying on its back (two trials, P2-P5: n=3 control, n=3 *Dmrt3*<sup>+/-</sup>, n=4, *Dmrt3*<sup>-/-</sup>, P6: n=5 control, n=7 *Dmrt3*<sup>+/-</sup>, n=6 *Dmrt3*<sup>-/-</sup>) was monitored daily. Weight-bearing locomotion (defined as the ability to move using all limbs without touching the ground surface with its belly), with or without tail pinch stimuli, was analysed between P5 and P7 (P5: n=5 control, n=7 *Dmrt3*<sup>+/-</sup>, n=8 *Dmrt3*<sup>-/-</sup>, P6-P7: n=6 control, n= 10 *Dmrt3*<sup>+/-</sup>, n=9 *Dmrt3*<sup>-/-</sup>). The experimenter was blind to genotype while performing and analysing experiments. Groups were analysed for statistical significance with Fisher's exact test.

### Airstepping

On postnatal (P) day P0.5-P1.5 (named P1 in figure) or P3.5-P4.5 (named P4 in figure) mice were placed in a soft fabric for holding the body. The four legs were freely hanging down and the head was freely movable. A high-speed camera (100 frames/s) recorded the movements from below, paws were painted to provide contrast. Leg movements were stimulated by finger pressure over the tail. 2x20 seconds were recorded for each mouse. Analysis: The video was played at ¼ of the normal speed and hind limbs were scored for the following parameters: Alternating step, Repeated one limb movement, Uncoordinated step or Synchronous step. The procedure was then repeated for the forelimbs. (P4: n=3 control, n=4 *Dmrt3*<sup>+/-</sup>, n=4, *Dmrt3*<sup>-/-</sup>, P1: n=4 control, n=4 *Dmrt3*<sup>+/-</sup>, n=4 *Dmrt3*<sup>-/-</sup>). Each parameter was then statistically tested using the Kruskal-Wallis test followed by Dunn's multiple comparison test. The experimenter was blind to genotype while performing and analysing experiments.

### Extracellular electrophysiology

P0-P2 mice were anesthetized with isoflurane and decapitated, eviscerated and submerged in ice-cold dissection buffer containing the following (in nM: 128 NaCl, 4.69 KCl, 25 NaHCO<sub>3</sub>, 1.18 KH<sub>2</sub>PO<sub>4</sub>, 3.5 MgSO<sub>4</sub>, 0.25 CaCl<sub>2</sub> and 22 D-Glucose; equilibrated with 95% O<sub>2</sub> and 5% CO<sub>2</sub>). The spinal cord was carefully dissected out of the spinal column and placed in a Sylgard-coated recording chamber. The spinal cord was then left for 30 min to recover continuously perfused with aCSF containing the following (in nM: 128 NaCl, 4.69 KCl, 25 NaHCO<sub>3</sub>, 1.18 KH<sub>2</sub>PO<sub>4</sub>, 1.25 MgSO<sub>4</sub>, 2.5 CaCl<sub>2</sub> and 22 D-Glucose; equilibrated with 95% O<sub>2</sub> and 5% CO<sub>2</sub>). Suction electrodes were attached to left and right L2 and L5 roots and locomotion was induced using 6 μM NMDA and 6 μM 5HT or 5 μM NMDA, 10 μM 5HT and 50 μM Dopa. Spinal cords were also treated with 500 μM Nipicotic acid and 500 μM Sarcosine or 10 μM Picrotoxin and 1 μM Strychnine. Fictive locomotion was analysed using the Matlab-based programs Spinalcore and Neurodata<sup>7,34</sup>. For analysis in Spinalcore the data was downsampled to 100 Hz and rectified. A Morlet wavelet transform was used to extract the phase and frequency from 400 seconds of recorded fictive locomotion. For analysis in Neurodata, 600 seconds of fictive locomotion was low-pass filtered at 5 Hz, rectified and high-pass filtered at 0.01 Hz. The resulting trace was analysed for burst, interburst and cycle period duration as previously described<sup>34</sup> and tested using the Kruskal-Wallis test followed by Dunn's multiple comparison test. The Neurodata analysis was also used to create the circular plots and subsequently tested with Rayleigh test (n=6 control, n=6 *Dmrt3*<sup>+/-</sup>, n=6 *Dmrt3*<sup>-/-</sup>). For treatment with nipicotic acid and sarcosine, n=3 *Dmrt3*<sup>-/-</sup>; for treatment with picrotoxin and strychnine, n=2 control and n=1 *Dmrt3*<sup>-/-</sup>.

### RNA *in situ* hybridization on mouse tissue

Spinal cord biopsies (1-2 cm) were immediately dissected and fixed for 48 h in 4% formaldehyde in PBS. Tissue was cryoprotected in 10% and 30% sucrose in PBS, embedded in TissueTec® and sectioned (E11-E12.5, 14 μm; P0-adult, 70 μm (floating sections)). *In situ* hybridization experiments were performed essentially as described<sup>35</sup> with an antisense DIG-labelled mRNA probe for mouse *DMRT3* covering 997 nucleotides of the transcript (from 1404 to 2401, NM\_177360.3), the *VIAAT* probe covers nucleotides 588-2072 (GeneID:18208/NM\_008744.2) and the *Vglut2* probe covers nucleotides 1616-2203 (NM\_080853.2). Hybridization was performed at 61°C O/N. Bound probe was detected using anti-DIG Fab fragments conjugated to alkaline phosphatase (Roche Diagnostics Scandinavia, Stockholm, Sweden) followed by incubation in NBT/BCIP (Roche Diagnostics) chromogenic substrate.

### Tracing

Spinal cords for tracing were prepared from mice at E15.5 and P0-P2. P0-P2 mice spinal cords were prepared as described earlier<sup>36</sup>. 3000 MW fluorescein-dextran-amine (FDA) (Invitrogen) was used for retrograde tracing of CINs as described previously<sup>37</sup>. Tracings on E15.5 embryos were performed essentially the same way, but the spinal cord remained within the vertebral column during tracer application and incubation. During dissection, animals were kept in ice-cold oxygenated (95% O<sub>2</sub>/5% CO<sub>2</sub>) artificial cerebrospinal fluid (aCSF [mM]: 128 NaCl, 4.69 KCl, 2.5 CaCl<sub>2</sub>, 1.25 MgSO<sub>4</sub>, 1.18 KH<sub>2</sub>PO<sub>4</sub>, 25 NaHCO<sub>3</sub>, 22 glucose, pH 7.4). Preparations were then incubated in a dark box in oxygenated aCSF at room temperature for 12-16h and then fixed in 4% paraformaldehyde (PFA) in 0.1 M PBS, pH 7.4 and stored dark at 4°C. P0-P1 spinal cords were stored for one week before cut into 60 μm thick transverse sections on a vibratome (Leica) and stored in the dark at -20°C until analysis. E15.5 samples for immunohistochemistry studies were fixed for 2 h and then transferred to 30% sucrose in PBS at 4°C overnight. The samples were embedded in TissueTec® and 12 μm sections were cut using a cryostat (CM1800, Leica), collected onto Superfrost slides (Menzel-Gläser) and stored in the dark at -80°C until usage for additional immunohistochemistry staining. Quantification of CINs and Wt1<sup>+</sup> neurons at E15.5 was done on 2 animals/genotype and the number of sections as indicated. Quantification of one segment (L2) projecting CIN at P0-P2 was done on 3 animals/genotype and the number of sections as indicated.

### Trans-synaptic tracing of interneurons

Attenuated pseudorabies virus strain Bartha (PRV Bartha) expressing enhanced green fluorescent protein (PRV152) was generously provided by Dr. Lynn Enquist (Princeton University, Princeton, NJ). PRV152 has been widely used for transneuronal tracing<sup>18,38</sup> as the cell body, nucleus and processes of the infected neurons are filled with EGFP. The virus was grown in pig kidney cells and the titers were set to a final concentration of  $4.86 \times 10^8$  plaque forming units (pfu/ $\mu$ l). The experiments were performed on P2 mice. All procedures were carried out according to Bio Safety level 2 conditions in accordance with the Work Environment Authority in Sweden. 24 h prior to the viral injection the mice were injected (IP, 50  $\mu$ g/g in 0.9% physiological saline) with a retrograde label Fluorogold (FG; Fluorochrome, Denver, CO) to produce global labelling of somatic motor neurons. The animals were anesthetised on ice and 3-4  $\mu$ l injections of PRV152 were made in multiple sites of the *tibialis anterior* (TA) or *gastrocnemius* (GC) muscle using a 10 $\mu$ l Hamilton syringe with a 34 gauge needle (NanoFil, World Precision Instruments). 38-40 h post-injection the mice were decapitated, the spinal cords dissected and immersed in 4% paraformaldehyde overnight. The following day the tissue was cryoprotected in 30% sucrose, cast frozen in O.C.T (Tissue Tek, Histolab, Gothenburg, Sweden) sectioned at 14  $\mu$ m on a cryostat and processed using immunohistochemistry as described above.

### Expression analysis using horse tissue

Spinal cord, muscle and testis samples were collected immediately after the horses were sacrificed and put into RNAlater or snap frozen in liquid nitrogen. RNAlater samples were kept at 4°C for 24 h followed by storage at -80°C until further processing. The spinal cord samples were extracted using the RNeasy Lipid Mini protocol (Qiagen) whereas the testis sample was processed with the regular RNeasy Mini kit (Qiagen). Samples used for qPCR were subjected to two on-column DNase treatments. The whole *DMRT3* transcript of wild-type and mutant horses was PCR amplified using 2  $\mu$ g of RNA that had been reverse transcribed using the RevertAid Premium First Strand cDNA synthesis kit (Fermentas; First strand cDNA synthesis protocol with a 1:1 mixture of random hexamer primers and oligo (dT)18 primer) using primers spanning exon-intron boundaries. The PCR mixture was as follows: 1x KAPA2G GC buffer with 1.5 mM MgCl<sub>2</sub>, 0.2 mM dNTPs, 0.2  $\mu$ M of each forward and reverse primer and 0.2U KAPA2G Robust Hotstart Polymerase (KAPA Biosystems).

RNA samples used for qPCR were subjected to an additional DNase treatment after extraction (DNAfree Kit, Ambion) to further minimize potential DNA contaminations. RNA samples were tested for absence of DNA contamination by performing qPCR on an aliquot of each sample that had not been reverse transcribed. Two  $\mu$ g of each DNA-free sample were reverse transcribed and used for qPCR. Primers and probes were designed using Primer3plus and evaluated for secondary structure using the online tool *mfold*. PCR efficiency and specificity of the primers were tested in a SYBRgreen assay (Applied Biosystems) first using a final concentration of 1X SYBRgreen PCR Master Mix and 1  $\mu$ M of each primer in a 10  $\mu$ l reaction. The standard curve, a 10X dilution series, was generated from cDNA obtained from testis. The standard curve was run on a 7900 HT Fast Real Time PCR. Primer pairs with a PCR efficiency between 92-102% and only one product in the melting curve analysis were chosen for the following genes: *DMRT3*, *ACTB* and *18s*<sup>39</sup>. The probes were labelled with 5'-6FAM and 3'-MGB (Applied Biosystems). The gene expression assay was performed using 2  $\mu$ l cDNA in a 10  $\mu$ l reaction volume (1x Gene expression Master Mix from Applied Biosystems, 0.8  $\mu$ M of each primer and 0.25  $\mu$ M labelled probe) with the following thermal cycling program: 50°C for 2 min, 95°C for 10 min, 95°C for 15 s and 60°C for 1 min. The PCR products were sequenced to verify their identity. The primer sequences are listed in table below.

### RNA *in situ* hybridization using horse tissue

Spinal cord biopsies (1–2 cm) were immediately dissected and fixed for 48 h in 4% formaldehyde in PBS. Tissue was cryoprotected in 10% and 30% sucrose in PBS, embedded using a TissueTec system (Sakura Fintek) and sectioned (25  $\mu$ m). *In situ* hybridization was performed essentially as described<sup>35</sup>, with an anti-sense DIG-labeled mRNA probe for horse *DMRT3* covering the whole transcript (1540 bp). Hybridization was performed at 61°C overnight. Detection of bound probe was done using anti-DIG Fab fragments conjugated to alkaline phosphatase (Roche Diagnostics), followed by NBT/BCIP (Roche Diagnostics) chromogenic substrate.

### Transfection experiments

Wild-type horse cDNA from testis was PCR amplified and cloned into a pcDNA3 vector (Invitrogen) containing an N-terminal myc-tag, using One Shot TOP10 chemically competent *E. coli* (Invitrogen). A truncated mutant form of *DMRT3* was generated by placing the reverse primer at the position of the nonsense mutation. Plasmid constructs were sequenced to verify a correct reading frame. The Plasmid Plus Maxi kit (Qiagen) were used to isolate DNA for EMSA and transfection experiments. eGFP-*DMRT3* fusion proteins were generated by ligating *DMRT3* in frame after a N-terminal eGFP in pcDNA3. Human glioma U251 cells were grown on coverslips and transfected with wild-type or mutant eGFP-*DMRT3* using Lipofectamine LTX (Life Technologies). Cells were fixed after 24 h and nuclei stained with DAPI and anti-*DMRT3* custom made in guinea pig antibody. Images were captured on a ZEISS LSM 510 META confocal microscope.

### Electrophoretic mobility shift assays (EMSA)

The oligonucleotide 5'-ggatccTCGAGAACAATGTAACAATTCGCCC-3' and its complementary sequence were annealed in 10 mM Tris pH 7.5, 1 mM EDTA, 50 mM KCl by firstly heating to 95°C for 2 min and thereafter cooled to 25°C (2 min/degree). The duplex was labelled with Klenow DNA polymerase and [ $\alpha$ -<sup>32</sup>P]-dCTP and purified using a Bio-Rad Micro Bio-Spin 30 column. *DMRT3* wild-type and mutant protein were produced by *in vitro*-translation using a TNT Quick Coupled Transcription/Translation System (Promega). EMSA was performed as described<sup>29</sup> with the following modifications; no plasmid DNA was added and 0.8  $\mu$ l *in vitro*-translated protein and 150x cold competitor were used. The reaction mixture was incubated in room temperature (RT) for 40 min. Gels were run at 150 V in RT. The same procedure was repeated for the *DMRT1* binding site using the oligonucleotide 5'-ggatccTCGAGATTTGATACATTGTTGC-3'.

### Imaging and picture processing

Bright field images were analyzed on a MZ16F dissection microscope with DFC300FX camera and FireCam software (Leica). Fluorescent and bright field images were viewed in an Olympus BX61WI microscope (Olympus, Sweden). For quantitative analyses of traced spinal cords, the application sites were identified and consecutive photographs were taken between the two application sites using the OptiGrid Grid Scan Confocal Unit (Qioptiq, Rochester, USA) and Volocity software (Improvision, Lexington, USA). Confocal images were captured on a ZEISS LSM 510 META confocal microscope and analysed using the ZEISS LSM510 image analysis software. Captured images were adjusted for brightness and contrast using Adobe Photoshop software.

### Statistical analyses

Data are expressed as mean  $\pm$  s.e.m. or as indicated. Groups were compared using one-way ANOVA or two-tailed two-sample equal variance student *t*-test (parametric data) and Kruskal-Wallis or Mann-Whitney U-test (non-parametric data) as determined by group and sample size as well as normal distribution test. Fisher's exact test was used when analysing categorical variables. Statistical testing was done using the GraphPad Prism software. Probability levels <0.05 were considered statistically significant. Rayleigh test was used to test whether the phase of recorded

signals were distributed non-uniformly in the circular phase space (0° - 360°). See each paragraph above for statistical details.

### Primers used for Sanger sequencing and quantitative PCR

Gene	Forward Primer (5'→3')	Reverse Primer (5'→3')	Specie	Probe	Method
<i>KANK1</i>	taatacgaactactatagggGAGAAGTGGCGGGGAATTAT	GCCCCACGACTTTATTCTCA	horse	-	Sequencing
<i>KANK1</i>	taatacgaactactatagggCAGAGGACACATCTGCCTGA	CAAAACCATCTGGAAATGG	horse	-	Sequencing
<i>KANK1</i>	taatacgaactactatagggGCTTCTGGCCTCACGAAATA	TGGCATGAAGACACCACAAT	horse	-	Sequencing
<i>KANK1</i>	taatacgaactactatagggAAGTCGACTGAGGGGCTCTT	ACCTTGGCCAGATAGGTTT	horse	-	Sequencing
<i>KANK1</i>	taatacgaactactatagggGCAACCCAGGTTATCCCTTT	TCACCTTCTGCACTTGCAAT	horse	-	Sequencing
<i>DMRT3</i>	CTCCTTCCAAGAAGCCTGTG	AGAGTCTGCGGAAAACCTCA	horse	-	Sequencing
<i>DMRT3</i>	GAGCACGCTCAGACCCTATC	AAAGAGCTCCGAAGTTTTTGC	horse	-	Sequencing
<i>DMRT3</i>	AGCTTTCGGGAGCTCAG	TCGATTCGGTCAATGAAAA	horse	-	Sequencing
<i>DMRT3</i>	GACCTTCAGCGACAAAAGACA	CCTTCATCCACAGACACGAC	horse	CGACCAGAGGAGCTCCCCAG	qPCR
<i>18s</i>	AGTCCCTGCCCTTTGTACACA	GATCCGAGGGCCTCACTAAAC	horse	CGCCCCTCGCTACTACCGATTGG	qPCR
<i>ACTB</i>	TGACCCCTCAAGTACCCCATC	TGCCAGATCTTCTCCATGTC	horse	AGCACGGCATCGTCACCAACT	qPCR
<i>Tubβ5</i>	AGTGCTCCTCTTCTACAG	TATCTCCGTGGTAAGTGC	mouse	-	qPCR
<i>Rpl19</i>	AATCGCCAATGCCAACTC	GGAATGGACAGTCACAGG	mouse	-	qPCR
<i>Gapdh</i>	GCCTTCGTTGTTCTACC	GCCTGCTTACCACCTTC	mouse	-	qPCR
<i>Dmrt3</i>	AGCGCAGCTTGCTAAACC	GAGCTCCTCTGATCGGTGTC	mouse	-	qPCR
<i>Dmrt1</i>	GCCCAGGAAGAAGAACTGG	GGGTTGCTGGCATTATTCTC	mouse	-	qPCR
<i>Dmrt2</i>	ATTTGATCGGAAAGCAGTG	ACTGACAGGCGGAGGTAGAG	mouse	-	qPCR
<i>Dmrt4</i>	TCGAGGTTTTCCAGCAAGAT	TCTCCACGGTCACATTACCC	mouse	-	qPCR

## Supplementary Notes

### Description of gaits

Gait, or the coordination of limb pattern used in locomotion, can be described by cadence (two-beat versus four-beat), foot-fall sequence, and timing (regular versus irregular, and lateral versus diagonal). Natural gaits of the domestic horse and other equids include the walk (four-beat, lateral gait at slow speed, ~6 km/h, with equal timing between footfalls), the trot (two-beat diagonal gait at intermediate speed, ~23 km/h) and the gallop (four beat, fast gait, ~40-50 km/h). A Standardbred trotter can trot at 50 km/h. The canter, a collected form of the gallop is also a naturally occurring gait distinguished from the gallop since collection results in a 3-beat cadence. Several horse breeds have been selected for the ability to perform gaits other than the walk, trot and gallop. These gaits are all performed at intermediate speed and often in place of the trot, although in 4- and 5-gaited Saddlebreds and 4- and 5-gaited Icelandic horses, alternate gaits are performed in addition to the trot<sup>40</sup>.

With the exception of pace, which is characterized by a two-beat cadence, alternate gaits performed by domestic horse breeds have a four-beat cadence, classified as “stepping” or “ambling” gaits due to a lack of an airborne (or suspension) phase<sup>41</sup>. In general the footfall sequence is left hind (LH), left fore (LF), right hind (RH) and right fore (RF). In the walk, the body is supported by two or three limbs at any given time, whereas in the various alternate gaits, the body may be supported by one and up to four limbs at a time<sup>41</sup>. Limb support sequences describe the pattern of limb support or the number of feet in contact with the ground at any given time (Supplementary Table 1). The gait of horses may have either a regular rhythm, in which the timing between each successive foot-fall is even or an irregular rhythm, in which the timing between successive foot-falls is not even. Gaits with irregular timing are characterized by having either lateral or diagonal couplets. With lateral couplets, the footfalls of ipsilateral feet (i.e. LH and LF) occur closely together in time, whereas with diagonal couplets foot-fall between the forelimb and the contralateral hind limb (i.e. RF and LH) are closely related in time<sup>42</sup>. Some alternate gaits are also distinguished by differences in foot placement<sup>43</sup> (i.e. over-reach in the running walk) or animation of joint motion<sup>44</sup> (i.e. “termino” or outward rolling motion of the forelimbs in the Peruvian Paso). Characteristics of the alternate four-beat gait(s) based on kinematic analysis of the breeds included in this study are outlined in Supplementary Table 1. To the authors’ knowledge, published descriptions of kinematic analysis of the gait of the Kentucky Mountain Saddle horse are not available.



## Supplementary References

28. Li, Q. *et al.* Nuclear localization, DNA binding and restricted expression in neural and germ cells of zebrafish Dmrt3. *Biol. Cell.* **100**, 453-463, (2008).
29. Murphy, M. W., Zarkower, D. & Bardwell, V. J. Vertebrate DM domain proteins bind similar DNA sequences and can heterodimerize on DNA. *BMC Mol. Biol.* **8**, 58, (2007).
30. Arnason, T. Genetic evaluation of Swedish standard-bred trotters for racing performance traits and racing status. *J. Anim. Breed. Genet.* **116**, 387-398 (1999).
31. Purcell, S. *et al.* PLINK: a tool set for whole-genome association and population-based linkage analyses. *Am. J. Hum. Genet.* **81**, 559-575 (2007).
32. DePristo, M. A. *et al.* A framework for variation discovery and genotyping using next-generation DNA sequencing data. *Nat. Genet.* **43**, 491-498, (2011).
33. Wang, K., Li, M. & Hakonarson, H. ANNOVAR: functional annotation of genetic variants from high-throughput sequencing data. *Nucleic Acids Res.* **38**, e164, doi:10.1093/nar/gkq603 (2010).
34. Zhang, Y. *et al.* V3 spinal neurons establish a robust and balanced locomotor rhythm during walking. *Neuron* **60**, 84-96, (2008).
35. Enjin, A. *et al.* Identification of novel spinal cholinergic genetic subtypes disclose Chodl and Pitx2 as markers for fast motor neurons and partition cells. *J. Comp. Neurol.* **518**, 2284-2304 (2010).
36. Wegmeyer, H. *et al.* EphA4-dependent axon guidance is mediated by the RacGAP alpha2-chimaerin. *Neuron* **55**, 756-767, (2007).
37. Eide, A. L. & Glover, J. C. Development of the longitudinal projection patterns of lumbar primary sensory afferents in the chicken embryo. *J. Comp. Neurol.* **353**, 247-259, (1995).
38. Card, J. P., Enquist, L. W. & Moore, R. Y. Neuroinvasiveness of pseudorabies virus injected intracerebrally is dependent on viral concentration and terminal field density. *J. Comp. Neurol.* **407**, 438-452 (1999).
39. Rosengren Pielberg, G. *et al.* A cis-acting regulatory mutation causes premature hair graying and susceptibility to melanoma in the horse. *Nat. Genet.* **40**, 1004-1009, (2008).
40. Zips, S., Peham, C., Scheidl, M., Licka, T. & Girtler, D. Motion pattern of the toelt of Icelandic horses at different speeds. *Equine Vet. J. Suppl.*, 109-111 (2001).
41. Nicodemus, M. C. & Clayton, H. M. Temporal variables of four-beat, stepping gaits of gaited horses. *Appl. Animal Beh. Sci.* **80**, 133-142 (2003).
42. Hildebrand, M. Symmetrical gaits of horses. *Science* **150**, 701-708 (1965).
43. Nicodemus, M. C., Holt, K. M. & Swartz, K. Relationship between velocity and temporal variables of the flat shod running walk. *Equine Vet. J. Suppl.*, 340-343 (2002).
44. Imus, B. *Heavenly Gaits: The Complete Guide to Gaited Riding Horses*. 11-24 (Crossover Publications, 1995).

## Supplementary Movie Legends

### **Supplementary Movie 1**

This movie shows a side view of a heterozygous (CA) Swedish Standardbred trotter that performs a fairly symmetric and normal trot stride as well as a very asymmetric stride. The horse is unable to stay consistently in trot at a speed where a wild-type horse would switch to canter. The slow-motion movie covers a period of about 5 seconds, during which 9 step-cycles are performed (QuickTime; 10 MB).

### **Supplementary Movie 2**

This movie shows a side-by-side view of wild-type and *Dmrt3*<sup>-/-</sup> mice (KO) mice during swimming. The last part of the movie is in 0.2x slow-motion. By following the hindlimbs during the course of the movie, fast short-stroke movements can be seen in the *Dmrt3*<sup>-/-</sup> mice (MPG; 9 MB).

### **Supplementary Movie 3**

This movie shows wild-type and *Dmrt3*<sup>-/-</sup> mice during treadmill locomotion. Parts of the movie are in 0.2x slow-motion. By following the limb movements during the course of the movie, differences in stride length can be seen as well as the difficulty for the *Dmrt3*<sup>-/-</sup> animals to manage higher treadmill velocities (MPG; 23 MB).

### **Supplementary Movie 4**

This movie shows wild-type and *Dmrt3*<sup>-/-</sup> mice during airstepping. Part of the movie, showing the P4 animals, is in slow-motion. By following the limb movements during the course of the movie, differences in coordination abilities can be seen in 4- and 1-day old wild-type and *Dmrt3*<sup>-/-</sup> mouse pups (MPG; 30 MB).